Journal of Photochemistry & Photobiology, A: Chemistry 461 (2025) 116174

Contents lists available at ScienceDirect

Journal of Photochemistry & Photobiology, A: Chemistry

journal homepage: www.elsevier.com/locate/jphotochem

The influence of microbial sources on astaxanthin implementation as sensitizer in dye sensitized solar cells (DSSCs)

Alessia Tropea [a], Donatella Spadaro [b,*], Ilaria Citro [b], Maurizio Lanza [b], Stefano Trocino [c], Roberta La Tella [a], Daniele Giuffrida [d], Cassamo U. Mussagy [e], Luigi Mondello [a,f], Giuseppe Calogero [b]

[a] Messina Institute of Technology C/o Department of Chemical, Biological, Pharmaceutical and Environmental Sciences, Former Veterinary School, University of Messina, Viale G. Palatucci Snc 98168 Messina, Italy
[b] Institute for Chemical and Physical Processes (IPCF)- National Research Council - Messina, Viale Ferdinando Stagno D'Alcontres, N. 37, 98158 Messina, Italy
[c] Institute for Advanced Energy Technologies "Nicola Giordano" (ITAE) - National Research Council (CNR), Via Salita S. Lucia Sopra Contesse, N. 5, 98126 Messina, Italy
[d] Department of Biomedical, Dental, Morphological and Functional Imaging Sciences, University of Messina, Via Consolare Valeria, 98125 Messina, Italy
[e] Escuela de Agronomía, Facultad de Ciencias Agrońomicas Y de Los Alimentos, Pontificia Universidad Católica de Valparaíso, Quillota 2260000, Chile
[f] Chromaleont S.r.l., C/o Department of Chemical, Biological, Pharmaceutical and Environmental Sciences, Former Veterinary School, University of Messina, Viale G. Palatucci Snc 98168 Messina, Italy

ARTICLE INFO

Keywords:
Dye sensitized solar cells (DSSCs)
Paracoccus carotinifaciens
Haematococcus pluvialis
Phaffia rhodozyma
Astaxanthin
Green energy

ABSTRACT

In the context of increasing the use of sustainable materials derived from renewable, non-toxic, and biocompatible sources, dyes obtained from microorganisms have garnered significant interest, particularly for clean energy applications. This study presents a novel comparison of astaxanthin produced from three different microbial sources for dye-sensitized solar cells (DSSCs) to evaluate their photovoltaic performance. Comprehensive characterization using multiple analytical techniques (HPLC-DAD-APCI-MS, UV–vis spectroscopy, scanning electron microscopy (SEM), IV measurements, and electrochemical impedance spectroscopy (EIS)) were carried out on pigments extracted from the microalga *Haematococcus pluvialis*, the yeast *Phaffia rhodozyma*, and the bacterium *Paracoccus carotinifaciens* to highlight the structural differences that influence the dyes' photoelectrochemical behavior. The results show that the DSSC based on the extract from *Paracoccus carotinifaciens* demonstrated the highest efficiency, recording a short-circuit current density (Jsc) of 2.86 mA/cm^2, an open-circuit voltage (Voc) of 0.419 V, a fill factor (FF) of 0.3, and a power conversion efficiency (PCE) of 0.36 %.

1. Introduction

Dyes play an important role in several industrial sectors, such as food, feed, medicine, nutraceutical, textile, and others. According to their sources, they can be classified as natural or synthetic. The implementation of the synthetic ones is currently generating several concerns because of their toxicity for the environment and for the human health [1], generating in the society a feeling knows as "*chemophobia*" [2]. Thus, searching for new natural dyes and pigments is an emerging challenge for scientists and for industries, focused on the increasing consumers demand for "*natural*". The main sources suitable for obtaining natural dyes for industrial applications are represented by plants and microorganisms. These last resulting more ideal than plants due to their easy availability for culturing, and the solubility and stability of their pigments [3,4,5]. Consequently, the ecofriendly and non-toxic microbial pigments represent a good natural alternative to synthetic dyes that find a massive resonance in several industrial sectors [5]. Because of the high production cost, to date the natural pigments market value is lower (24 %) than the one of the synthetic dyes (76 %) [6,7]. Among the several classes of natural microbial pigments, the most employed in several industrial sectors, are represented by carotenoids due to their positive biological effects [6,8,9]. Astaxanthin, whose global market is expected to reach $ 3.4 billion by 2030, is the main carotenoids produced and widely used in food, feed, cosmetic, nutraceutical and pharmaceutical industries [10]. Currently, the interest towards this carotenoid is gaining more attraction due to its possible

* Corresponding author.
E-mail address: donatella.spadaro@cnr.it (D. Spadaro).

https://doi.org/10.1016/j.jphotochem.2024.116174
Received 16 October 2024; Received in revised form 7 November 2024; Accepted 21 November 2024
Available online 23 November 2024

implementation in further industrial sectors, mainly in the energy one as photosensitizer [11]. Searching for efficient technologies based on the application of molecules able to convert the solar energy into electricity without harming the environment is one of the most actual challenges to be addressed due to the rapid global population and urbanization growth [12]. Photovoltaic cells can convert sunlight into electricity, and a specific type of cells, known as dye-sensitized solar cells (DSSCs), have shown great promise. Natural dyes and their organic derivatives are attractive options for environmentally friendly solar cells due to their non-toxic, affordable, renewable, and abundant characteristics. As a result, researchers have extensively explored the possibility of harnessing solar energy using natural dyes, which offers a cost-effective and straightforward approach that avoids the production of hazardous waste through chemical and physical processing methods [13]. In this context the implementation of astaxanthin as photosensitizer for DSSCs development can represent a possible solution.

Astaxanthin (3,3′-Dihydroxy-β,β-carotene-4,4-dione, AXT) is a lipid-soluble red–orange pigment, containing a long conjugated double bonds chain and two terminal β-ring systems bearing hydroxyl and carbonyl groups. These groups make astaxanthin a good sensitizer in DSSCs, as they allow it to interact with the TiO_2 surface through chelation to the Ti4 + site, enabling the injection of electrons into the conduction band of TiO_2 [14]. Note that, astaxanthin is a natural pigment (colorant) but can be referred to as a dye due to its use in applications such as DSSCs, where its properties as a colorant are utilized.

To date, the most encouraging and efficient source of astaxanthin is represented by microorganisms, and the most promising are the microalga *Haematococcus pluvialis*, the yeast *Phaffia rhodozyma,* (also known as *Xanthophyllomyces dendrorhous*) and the bacterium *Paracoccus carotinifaciens* [10,15,16].

As already pointed out in previous literature, several advantages have been demonstrated for natural microbial pigment implementation for DSSCs development over the implementation of other synthetic or natural pigments [17–36]. Microbes show a fast growth rate, and they can be cultivated on a large scale in bioreactors throughout the all the year, being not affected by season. The pigments produced are usually non-carcinogenic, non-toxic and fully biodegradable, making them eco-friendly alternatives to the synthetic pigments. Moreover, microbial pigments are produced mainly as a mixture of correlated compounds, strictly dependent to the producer microorganism, resulting in a capability of absorbing most of the light energy due to their wide absorption spectrum, thus affecting the final device performance. Finally, the mixture compound ratio is affected by the cultivation strategies, resulting in the possibility to control the main pigments produced by modifying the culture conditions [3,37,38,39,40].

Previous studies have been carried out on the DSSCs development by using *Haematococcus pluvialis* astaxanthin-rich extract as photosensitizer [11,41,42], whereas to the best of our knowledge no previous research on DSSCs development by using extracts obtained from other producing astaxanthin microorganisms have been carried out.

This study aimed to compare the implementation of microbial astaxanthin-rich extracts (ARE) obtained by the three main microbial sources, for the DSSCs development, in order to highlight the importance of investigating how the DSSCs performance can be affected by the complexity of the mixture in dyes composition, giving rise to an innate co-sensitization process. The microorganisms employed for this purpose were *Haematococcus pluvialis*, *Phaffia rhodozyma* and *Paracoccus carotinifaciens,* all selected for their high ARE production capacity.

2. Experimental section

2.1. Biological materials

In this study the biomasses from three different microorganisms have been employed. *Paracoccus carotinifaciens*, a Gram-negative marine bacterium commercialized as Panaferd®, and *Haematococcus pluvialis*, a microalga commercialized as NatAxtin®, both donated by ENEOS group (Tokyo, Japan) and Atacamabio (Tarapacá, Chile), respectively. Whereas *Phaffia rhodozyma* biomass NRRL Y-17268 was obtained by the yeast strain cultivation following the methodology described in previous work by [15].

2.2. Pigments extraction procedures for HPLC analyses and DSSCs implementation

The microbial dried biomasses (1 g each) have been extracted by successive extractions using 5 mL of acetone [15,43], repeated until the biomasses become fully decolorized. Acetone addition was followed by 5 min stirring at 65 °C and 300 rpm for enhancing the extraction efficiency. Samples were centrifuged (2500 xg for 10 min at 25 °C) in a Minicen Orto Alresa centrifuge (Madrid, Spain), and the astaxanthin-rich supernatant combined, concentrated and used for chemical characterization by HPLC. Each ARE has been employed for DSSCs implementation. After acetone removing by using a rotary evaporator at 65 °C and 100 mbar (Hei-VAP Precision, Heidolph Instruments GmbH &Co, Schwabach), the pigments extracts have been resuspended in EtOH, to obtain the dyes solutions to be tested as photosynthesizes (Fig. 1).

2.3. Analytical conditions for pigments extracts characterization

The pigments extracted and dissolved in acetone were filtered through PTFE syringe filter (0.45 μm) before HPLC analyses for carotenoids characterization. *Paracoccus carotinifaciens* HPLC analyses were carried out using a Shimadzu (Kyoto, Japan) instrument, consisted of a binary solvent pump LC-30 AD, a photodiode array detector (PDA) SPD-M30A serially coupled to an LCMS-8060 spectrometer via an atmospheric pressure chemical ionization (APCI) source operating in both positive and negative ionization mode. Chromatographic separation was performed on a YMC C30-column (250 x 4.6 mm, 5 mm); the mobile phases were as follows: methanol:MTBE:water (83:15:2,v/v/v; eluent A) and methanol: MTBE:water (8:90:2,v/v/v; eluent B). The gradient was from 0 to 20 % B in 20 min, from 20 to 50 % B in 60 min, from 50 to 100 % B in 65 min, hold for 5 min at 100 % B; back to 0 % in 5 min. The flow rate was 0.8 mL/min, the column oven was set at 30 °C, and the injection volumes were 20 μL. Shimadzu Lab Solution Software (Shimadzu, Kyoto, Japan) was used for data acquisition and handling. The wavelength range was 200–700 nm, and the chromatograms were extracted at 450 nm (sampling frequency: 4.1667 Hz; time constant: 0.480 s). MS parameters (APCI both positive and negative) were set as follows: *m/z* range, 100–700; scan speed, 3333 u/s; nebulizing gas (N2) flow rate, 4 L/min; event time: 0.5 s; detector voltage, 0.5 kV; interface temperature, 350 °C; DL (desolvation line) temperature, 300 °C; heat block temperature, 300 °C; drying gas flow, 5 mL/min [35].

Haematococcus pluvialis and *Phaffia rhodozyma* carotenoids determinations were carried out as above described, with slight analytical

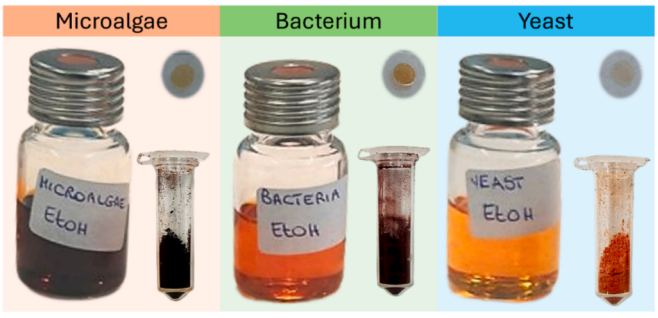

Fig. 1. Microbial biomasses (in Eppendorf tubes) and dye solutions (in bottles and cuvettes) tested as photosynthesizers. Microalgae refer to *Haematococcus pluvialis*, bacterium refers to *Paracoccus carotinifaciens,* and yeast refers to *Phaffia rhodozyma.*

method modification. The gradient elution was: 0 min 0 % B; 30 min 34 % B; held min at 34 %; 50 min 56 % B; held 5 min at 56 %; 70 min 78 % B; 75 min 100 % B; 85 min 0 % B. Whereas the *m/z* range was set at 100–1700 nm.

Carotenoids identification was accomplished by comparing retention times, DAD, and MS spectra obtained from the analyzed samples with those reported in the literature.

2.4. Sample preparation for UV analyses

Ultraviolet–Visible Spectroscopy (UV/vis) analyses were carried out by using a 190–1000 nm scan of the pigment solutions by using a UV2700 spectrophotometer (Shimadzu, Kyoto, Japan). The maximum absorption peaks of the single pigments as well as of the pigment's combinations, were identified. The solvents used for the pigment resuspension, ethanol, were used as blank.

2.5. Manufacturing procedure and operating principles of the devices

The DSSCs structure is significantly different from traditional solid-state junction devices by substituting the semiconductor contact phase with a liquid, gel, or solid electrolyte. A typical DSSC assembles four elements: working electrode (WE), sensitizer (dye), redox-mediator (electrolyte), and counter-electrode (CE). The photoanode consists of a monolayer of sensitizing dye adsorbed onto a mesoporous oxide layer of TiO_2. This layer inside the cell reacts with the I_3^-/I^- redox couple in the electrolyte solution, which acts as an electron donor for the oxidized dye molecules.

Upon exposure to light, the dye molecules absorb photons, exciting an electron from its highest occupied molecular orbital (HOMO) to its lowest unoccupied molecular orbital (LUMO), which has an energy level above the conduction band (CB) edge of the semiconductor. The excited electrons are subsequently injected into the CB of the semiconductor, where they diffuse towards the transparent conductive oxide (TCO) layer, made of fluorine tin oxide (FTO). The electrons then flow through the external circuit and return to the cell at the counter electrode (CE), glass surface coated with platinum (Pt). At the end of the process, the reducing agent diffuses from the CE into the semiconductor film to regenerate the oxidized dye back to its original state, completing the oxidation/reduction cycle [12].

DSSCs were fabricated following the procedure used in previous study carried out by Tropea *et al.* [35,36]. A pre-treated fluorine-doped tin oxide (FTO) glass plate with aqueous $TiCl_4$ and sintered at 500 °C for 30 min, was coated by mesoporous titanium oxide paste (18NR-T, Greatcell Solar) using screen-printing method and then dried for 6 min. at 125 °C. This coating–drying procedure was repeated to increase the thickness up to approximately 14 μm, measured with a profilometer, with an active area of around 0.181 cm^2. The photoanode thickness was measured using a surface profiler DektakXT (Bruker) equipped with a diamond-tipped stylus (radius of 2 m) and selecting a vertical scan range of 524 m, a scan length of 6000 m, and a stylus force of 1 mg. Each measure was verified with different runs acquired with different starting positions by translating the sample. SEM characterization was performed by a Zeiss Supra 25 Scanning Electron Microscope (SEM) with a Schottky field emission gun. The acceleration voltage can be varied in the 0.1–30 kV range.

The electrode was gradually heated under an air flow at 325 °C for 5 min., at 375 °C for 5 min, at 450 °C for 15 min., and at 500 °C for 15 min. The TiO_2 film was then immersed in a $TiCl_4$ solution to form an upper blocking layer.

Photoanodes were realized for adsorption of TiO_2 film for 24 h in sensitizer solutions obtained by different microbial sources ARE extracted from *Paracoccus carotinifaciens, Haematococcus pluvialis and Phaffia rhodozyma* and dispersed in ethanol, following a procedure extensively tested and reported in previous works [44].

The counter-electrode (CE) was prepared depositing on the FTO-glass plate with a drilled hole, a Pt transparent catalyst (PT1, Greatcell Solar) through doctor blade method and heating at 550 °C for 30 min.

The devices were assembled sealing the photoanodes with the CE using a thermopress with a Surlyn gasket (Meltonix 1170–25, Solaronix SA) as shown in scheme 1.

The electrolyte, AS8* (LiI 0.8 M, I2 0.05 M in AN:VN 85:15), was introduced into the cell through backfilling under vacuum and the hole sealed with adhesive tape. Device's behavior was investigated in relation to different microbial source pigments.

The photovoltaic performances of a DSSC are expressed by the following mathematical expressions used for the determination of power conversion efficiency:

$$PCE = FF\, J_{sc} V_{oc}$$

where PCE (%) is the power conversion efficiency, J_{SC} (mA/cm ^{2}) is the short circuit current, V_{OC} (V) is the open circuit voltage, FF is the fill factor. These parameters strongly depend on factors such as the structure of the dye used, the geometry of the device, by the type of sealing and the interaction at the photoanode interface [45,46].

A digital Keithley 236 multimeter connected to a PC and controlled by a homemade program was used to obtain the current–voltage (I-V) curves for the constructed devices. Simulated sunlight irradiation was provided by a LOT-Oriel solar simulator (Model LS0100-1000, 300 W Xe-Arc lamp, powered by LSN251 power supply equipped with AM 1.5 filter, 100 mW/cm^2).

The DSSCs were connected to an Autolab Potentiostat/Galvanostat (Metrohm) equipped with a frequency response analyzer (FRA). EIS experiments were conducted over a frequency range of 100 kHz to 100 mHz at 0.45 V (0.01 Vrms) to compare the different performances. Data fitting for the extraction of the elements of the equivalent electrical circuit was carried out using NOVA software (Metrohm).

3. Results and discussion

3.1. HPLC characterization for astaxanthin-rich extracts identification

The carotenoids composition of the extracts of *P. carotinifaciens*, *H. pluvialis* and *P. rhodozyma* are reported in Table 1. The main pigment detected in microbial biomass was represented by astaxanthin (Fig. 2) and the overall prevailing carotenoids where all bearing keto groups in their structures.

The compounds identified in *P. carotinifaciens* extract were, according to elution order, 13/*cis*-Astaxanthin (4.35 %), All-E-Astaxanthin (64.45 %), Adonixanthin (7.01 %), Adonirubin (19.89 %), and Canthaxantin (4.29 %). *H. pluvialis* biomass carotenoids extract were represented, according to their elution order, by Astaxanthin, Lutein, Adonirubin, Canthaxanthin, Astaxanthin monoesters (C18:4; C18:3; C18:2; C18:1; C18:0; C16:0), and Astaxanthin diesters (C18:2/C18:3;

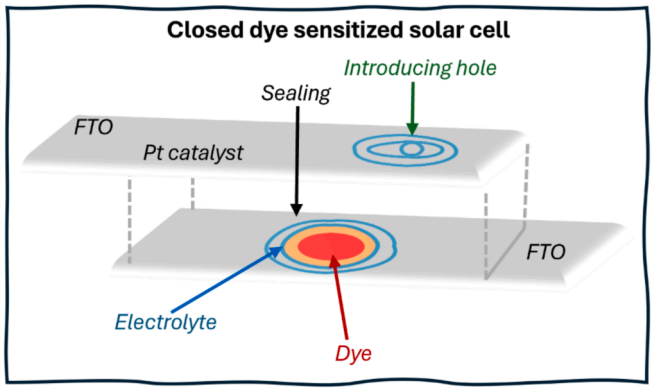

Scheme 1. Design of a closed dye sensitized solar cell.

Table 1
Overall compounds detected by HPLC-PDA-APCI/MS in microbial pigments extracts.

	Compound	Rt	PDA, l nm	APCI/MS (+) positive (−) negative	Tentative Identification	Carotenoid Composition (%)
Paracoccus carotinifaciens	1	11.3	370, 466	597 $[M+H]^+$; 596 $[M-H]^-$	13/*cis*-Astaxanthin	4.35
	2	12.6	477	597 $[M+H]^+$; 596 $[M-H]^-$	All-*E*-Astaxanthin	64.45
	3	14.7	466	583 $[M+H]^+$; 582 $[M-H]^-$	Adonixanthin	7.01
	4	15.3	476	581 $[M+H]^+$; 580 $[M-H]^-$	Adonirubin	19.89
	5	18.4	474	565 $[M+H]^+$; 564 $[M-H]^-$	Canthaxanthin	4.29
Haematococcus pluvialis	1	11.1	436	597 $[M+H]^+$; 596 $[M-H]^-$	Di-*cis*-astaxanthin	0.60
	2	12.4	475	597 $[M+H]^+$; 596 $[M-H]^-$	All-*E*-Astaxanthin	3.88
	3	14.3	421, 444, 472	551 $[M+H]^+$; 568 $[M-H]^-$	Lutein	4
	4	14.9	474	581 $[M+H]^+$; 580 $[M-H]^-$	Adonirubin	0.39
	5	15.4	466	597 $[M+H]^+$; 596 $[M-H]^-$	9-*cis*-Astaxanthin	0.45
	6	17.8	474	565 $[M+H]^+$; 564 $[M-H]^-$	Canthaxanthin	1.27
	7	24.3	475	855 $[M+H]^+$; 854 $[M-H]^-$	Astaxanthin-C18:4	3.08
	8	26.2	477	857 $[M+H]^+$; 856 $[M-H]^-$	Astaxanthin-C18:3	15.07
	9	27.6	477	859 $[M+H]^+$; 858 $[M-H]^-$	Astaxanthin-C18:2	14.83
	10	29.9	476	861 $[M+H]^+$; 860 $[M-H]^-$	Astaxanthin-C18:1	14.16
	11	32.5	477	835 $[M+H]^+$; 834 $[M-H]^-$	Astaxanthin-C16:0	19.16
	12	37.2	477	863 $[M+H]^+$; 862 $[M-H]^-$	Astaxanthin-C18:0	1.65
	13	41.7	477	1119 $[M+H]^+$; 1118 $[M-H]^-$	Astaxanthin diester-C18:2/C18:3	0.88
	14	46	477	1097 $[M+H]^+$; 1096 $[M-H]^-$	Astaxanthin diester-C18:2/C16:1	1.06
	15	47.2	477	1098 $[M+H]^+$; 1097 $[M-H]^-$	Astaxanthin diester-C18:2/C16:0	1.04
	16	48.8	477	1100 $[M+H]^+$; 1099 $[M-H]^-$	Astaxanthin diester-C16:1/C18:1	0.81
	17	50.3	477	1074 $[M+H]^+$; 1073 $[M-H]^-$	Astaxanthin diester-C16:0/C18:0	0.82
Phaffia rhodozyma	1	12.4	477	597 $[M+H]^+$; 596[M-H]$^-$	All-*E*-Astaxanthin	41.77
	2	15	474	581 $[M+H]^+$; 580 $[M-H]^-$	Adonirubin	13.59
	3	34.9	451, 477	550[M+H]$^+$; 530[M-H]$^-$	n.i.	24.62

n.i.: Not Identified.

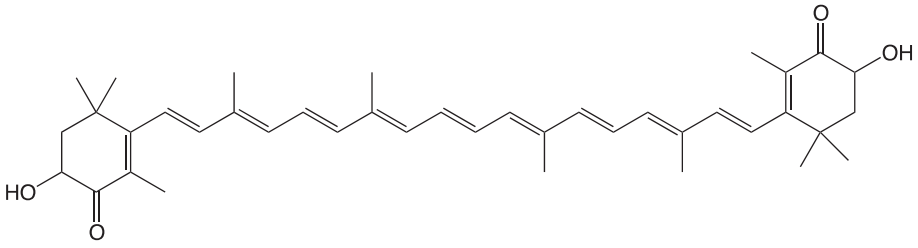

Fig. 2. Astaxanthin chemical structure.

C18:2/C16:1; C18:2/C16:0; C16:1/C18:1; C16:0/C18:0). Among these identified carotenoids, the main representatives were free form of Astaxanthin (3.88 %) and its esterified forms Astaxanthin-C18:3 (15.07 %), Astaxanthin-C18:2 (14.83 %), Astaxanthin-C18:1 (14.16 %), and Astaxanthin-C16:0 (19.16 %).

P. rhodozyma biomass carotenoids extract mainly consisted of the Astaxanthin (41.77 %) and Adonirubin (13.59 %). In this extract, one compound has not been identified since its PDA and MS spectra did not allow to tentatively determine a corresponding known structure.

The three investigated microorganisms, (*P. carotinifaciens, H. pluvialis and P. rhodozyma*) are known to produce respectively AXT having the 3S,3′S configuration, the 3S,3′S configuration esterified with fatty acids, and the 3R,3′R configuration.

3.2. DSSCs spectrophotometric and morphological characterization

The UV vis characterization (Fig. 3) for all pigments agrees with the results obtained from the chromatographic analysis and compounds identifications reported in Table 1. The dyes obtained from different microorganisms, shown a strong absorption in the visible region, and particularly the bands relating to astaxanthin; the free hydroxyl groups are able to make a strong link with the surface of the mesoporous titanium oxide film [44,47]. The bacterium *P. carotinifaciens* almost

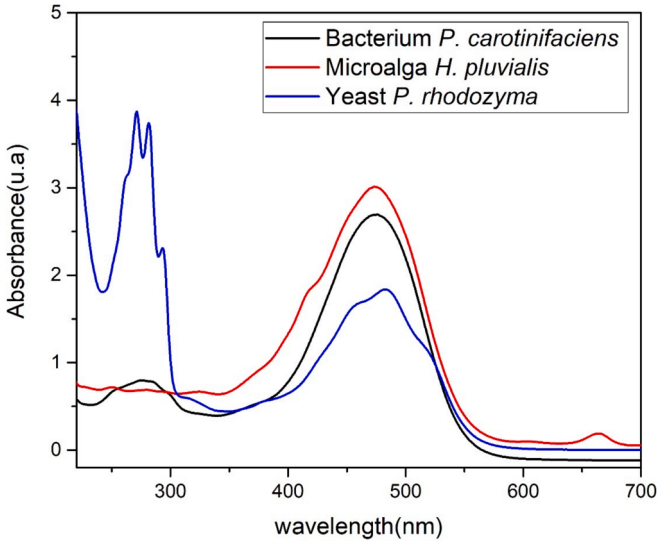

Fig. 3. Solutions absorbance spectra of different pigments in ethanol. Microalga refers to *H. pluvialis*, bacterium refers to *P. carotinifaciens,* and yeast refers to *P. rhodozyma.*

exclusively shown a typical absorption band centered around 477 nm due to the contributions of free astaxanthin [48,49]. The same absorption band was observed in the UV–vis spectra of the extract from *H. pluvialis* due to the occurrence of both free and fatty acids esterified astaxanthin together with a small contribution at 665 nm which could be associated to the presence of residual chlorophyll *a* coming from the extraction method [50].

Whereas, regarding the yeast *P. rhodozyma*, beside the astaxanthin absorption band, it was also observed a band in the UV spectrum absorbing at 270, 281, 293 nm [51], which did not contribute to the efficiency of the dye in DSSCs because of the glass inability in absorbing the visible light, while it is absorbing ultraviolet rays. These contributions were probably linked to the presence of a compound, not identified in the HPLC analysis, that has a conjugated system in its structure that absorbs in the UVB region (280–320 nm) [52]. These results were reflected in the photoelectrochemical behavior of the dye inside the device because different compounds contribute to the main band which leads to an improvement in photovoltaic performance as in a co-sensitization process [36].

The films obtained through this procedure were well homogeneous with a thickness of 14 μm as shown in Fig. 4a and the size of the titanium oxide particles were of the order of 20 nm as shown in Fig. 4b. These morphological characteristics were suitable to create a good interaction at the interface with the dye. Representative absorbance spectra of astaxanthin from P. carotinifaciens in ethanol and after absorption on nanostructured titanium oxide film are reported in Fig. 5.. The anchoring of the dye to the surface of the film was evident from the shift in the absorption spectrum.

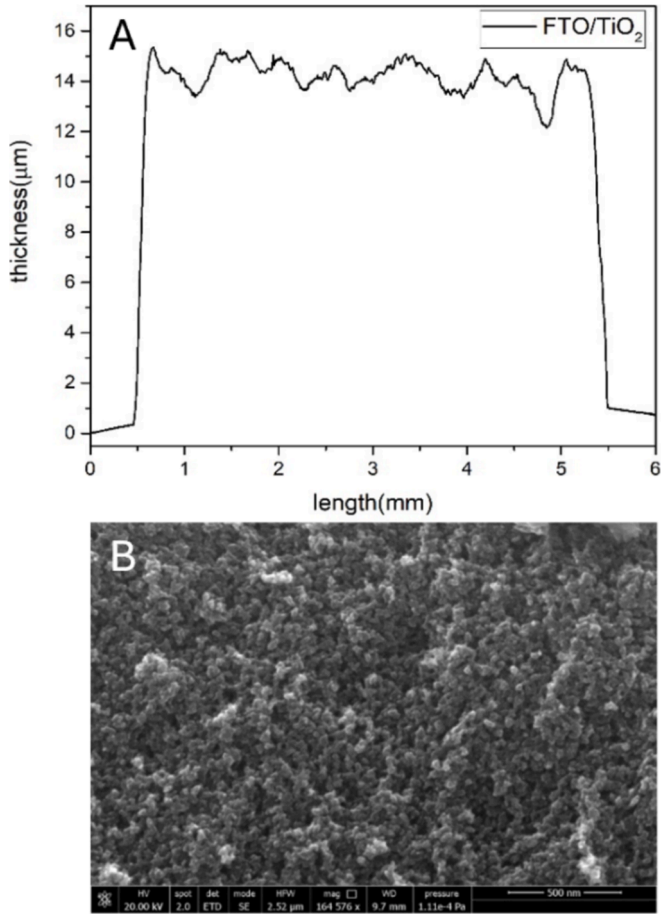

Fig. 4. Profile a) and b) SEM micrograph of the nanostructured titanium oxide film deposited on FTO.

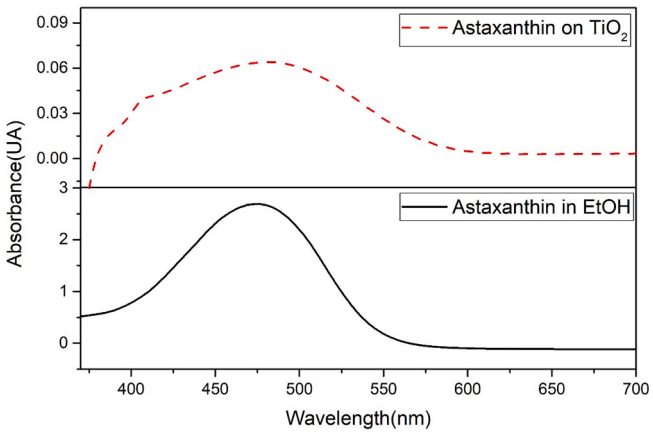

Fig. 5. Absorbance spectra of astaxanthin from *P. carotinifaciens* in ethanol and after absorption on nanostructured titanium oxide film.

3.3. DSSCs photoelectrochemical performances

For this study three samples were assembled using microorganism extracts as dyes to evaluate the influence of the percentage of free non-esterified astaxanthin present in bacterium *P. carotinifaciens*, microalgae *H. pluvialis* and yeast *P. rhodozyma* on photovoltaic performances. Each IV measurement was carried out and repeated three times. From a structural point of view, it is known from the literature that the presence of compounds in a dye that possess functional groups such as carbonyls, carboxylics and hydroxyls, leads to a better surface bond with the mesoporous structure of the semiconductor film [46,53]. As a result, the number of photons injected by the dye molecule into the conduction band of the semiconductor after absorption, will be significantly higher. The results obtained for the photovoltaic parameters Voc, Jsc, FF and PCE for the three different microorganisms are reported in Fig. 6 and in Table 2, considering the average and standard deviation values on 3 samples. Among the three microorganisms' extracts employed, the best performance in terms of density current and therefore efficiency has been achieved by the bacterium extract. This behavior can be ascribable to the total free astaxanthin, as previously described in the chromatographic characterization, and to the amount of pigment characterized by the free OH, that allowed it to interact with the anode surface [46]; moreover, in the bacterium extract a relatively high percentage of adonirubin, also bearing a free hydroxy group, was here reported.

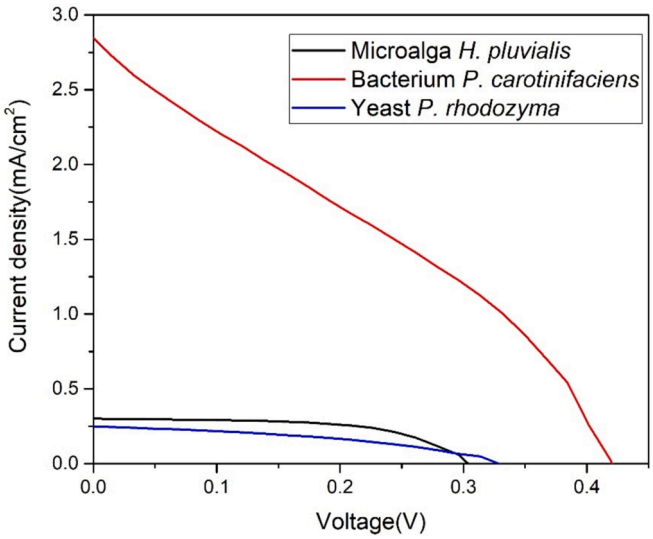

Fig. 6. IV curves of DSSCs based on microbial ARE pigments.

Table 2
Values of open-circuit voltage (V_{OC}), short-circuit photocurrent density (J_{SC}), fill factor (FF) and power conversion efficiency (PCE) related to different dyes-producing microorganisms. Average and standard deviation values are calculated over a set of 3 cells repeated three times.

Dyes-procuding microorganisms	Jsc (mA/cm^2)	Voc (V)	FF	PCE (%)	Ref
Bacterium *P. carotinifaciens*	2.86 ± 0.03	0.41 ± 0.05	0.3 ± 0.02	**0.36 ± 0.04**	This work
Yeast *P. rhodozyma*	0.25 ± 0.02	0.36 ± 0.03	0.48 ± 0.01	0.04 ± 0.02	This work
Microalga *H. pluvialis*	0.30 ± 0.01	0.29 ± 0.02	0.60 ± 0.01	0.05 ± 0.02	This work
Fungus *Monascus red*	1.23	0.75	0.72	0.66	34
Fungus *Talaromyces atroroseus GH2*	0.99 ± 0.01	0.35 ± 0.01	0.62 ± 0.01	0.11 ± 0.01	35
Bacterium *Escherichia coli*	0.686	0.29	––	0.06	22
Bacterium *Hymenobacter* sp.	0.20 ± 0.012	0.43 ± 0.05	0.37	0.03	19
Bacterium *Hymenobacter* sp.	0.12	0.46	0.51	0.03	18
Bacterium *Chryseobacterium* sp	0.13 ± 0.006	0.55 ± 0.02	0.48	0.03	19
Bacterium *Arthrobacter bussei* CP30	0.12 ± 0.01	0.29 ± 0.04	0.50 ± 0.01	0.01 ± 0.02	36
Bacterium *Paracoccus bogoriensis* BOG6	0.17 ± 0.01	0.34 ± 0.01	0.56 ± 0.02	0.03 ± 0.01	36
Bacterium *Serratia marcescens* 11E	0.096	0.56	0.60	0.032	24
Bacterium *Streptomyces fildesensis.*	0.091	0.49	0.579	0.026	20
Microalga *Chlorella* sp. PP1	0.012	0.23	0.35	0.001	28
Microalga *Scenedesmus obliquus*	0.61	0.44	0.70	0.19	31
Microalga *Haematococcus pluvialis*	0.313 ± 0.005	0.449 ± 0.002	0.72 ± 0.44	0.10 ± 0.004	11
Co-sensitization					
Talaromyces atroroseus GH2_ Arthrobacter bussei CP30	0.29 ± 0.04	0.32 ± 0.02	0.62 ± 0.02	0.06 ± 0.03	36
Talaromyces atroroseus GH2_ Paracoccus bogoriensis BOG6	1.59 ± 0.06	0.35 ± 0.03	0.62 ± 0.01	0.34 ± 0.04	36
Arthrobacter bussei CP30_ *Paracoccus bogoriensis* BOG6	0.27 ± 0.06	0.35 ± 0.05	0.52 ± 0.02	0.05 ± 0.04	36
Halobacterium salinarum, NRC-1_Halobacterium salinarum R1	0.45	0.57	0.62	0.16	25

Although a large amount of astaxanthin was also identified in *H. pluvialis* extracts, here the hydroxyl group esterification did not allow the adsorption of the dye on the surface. The presence of a conjugated double bonds system was evident in the UV spectrum of the yeast, which leads to an increase in Voc as they reduce the phenomenon of recombination and involves fast electron transfer as will be discussed by impedance spectroscopy measurements [13]. The best device performance was obtained by using the bacterium *P. carotinifaciens* ARE extract, that gave the highest PCE value of 0.36 ± 0.04. This percentage of efficiency represent an interesting result if compared with previous literature regarding the implementation of microbial dyes for the development of DSSCs [11,18,19,20,22,24,25,28,31,34,35,36]. As reported in Table 2, it is possible to notice that the results obtained in this study are higher than the ones obtained both when dyes were extracted from a single microorganism or when dyes were obtained from different microorganisms and used in co-sensitization mode, in the same operative conditions. In this regard, comparable results have been previously reached by using the extracts obtained from *Talaromyces atroroseus GH2* and *Paracoccus bogoriensis* BOG6 where the PCE was 0.34 ± 0.04 [36].

Whereas, higher efficiency values have been obtained in other studies based on the application of different dyes characterized by a higher number of functional groups (CO, OH, etc.) suitable for bonding with the surface of the anode, and based on the employment of DMSO in the electrolyte [22].

Electrochemical Impedance Spectroscopy (EIS) is an advanced and essential analytical technique widely utilized in studying and optimizing DSSCs. This technique provides a deep understanding of the intricate electrochemical processes that govern the performance of DSSCs by measuring the cell's impedance across a range of frequencies, from mega-Hertz to milli-Hertz. EIS involves applying a small AC voltage perturbation to the solar cell and measuring the resulting AC response (current) [54,55,56]. The data obtained is often represented in Nyquist and Bode plots, which help deconvolute various impedance contributions within the cell.

The Nyquist plot, a common output of EIS, typically displays a series of semicircles and lines corresponding to different electrochemical processes. The high-frequency intercept of the Nyquist plot represents the series resistance (R_S), which includes contributions from the conductive substrates, interconnections and electrolyte. The semicircle in the mid-frequency region is indicative of the charge transfer resistance (R_{CT}) at the photoanode/electrolyte interface, reflecting the efficiency with which electrons are injected from the organic dye molecules into the photoanode. Additionally, the low-frequency tail of the Nyquist plot often illustrates the diffusion resistance (R_{DIFF}) within the electrolyte and the chemical capacitance (C_μ), associated with the density of states and the position of the Fermi level in the semiconductor [57,58,59,60].

For DSSCs incorporating organic dyes, EIS is particularly instrumental due to the unique electrochemical properties these natural dyes bring. These biological sources offer complex molecular structures and diverse functional groups, which can significantly impact on the charge transfer dynamics and overall cell performance [35,36]. EIS helps elucidate how these natural dyes interact with the photoanode, their electron injection efficiencies, and the recombination dynamics at the dye/semiconductor interface. Furthermore, EIS provides insights into the stability and degradation mechanisms of DSSCs over time. By conducting impedance measurements at different intervals during the operational life of the cell, it is possible to monitor changes in resistance and capacitance, thereby identifying potential degradation pathways and to study the structure of the photoanode, electrolyte, and counter electrode to minimize resistive losses and maximize charge collection efficiency.

In the specific case, DSSCs based on microalgae, bacterium, and yeast astaxanthin-rich extracts, had the same R_S series resistance because the electrolyte, conductive substrate, and interconnections did not vary from case to case. The value of Rs identified by Nyquist diagram analysis, shown in Fig. 7, is 1.5 Ω ^{2} (Table 3). On the other hand, analysis of the charge transfer part of the same graph shown completely different total resistance (R_T) values. At low frequency the samples shown a distinct diffusion pattern; in fact, the total resistances were on the order of 18 kΩ cm^2 and 22 kΩ cm^2 for microalgae and bacteria, respectively (Table 3). These relatively high R_{CT} values indicated that the electron transfer process at the photoanode/electrolyte interface might be less efficient, potentially due to the complex molecular structure of the dye, which could lead to slower electron injection rates or higher recombination losses.

In the case of yeast, instead, the total resistance was significantly lower, at around 140 Ω ^{2} (Table 3). This indicates a much more efficient electron transfer process at the photoanode/electrolyte interface, suggesting that the molecular structure of the yeast dye was more conducive to rapid electron injection and lower recombination rates as discussed in section related to UV–Vis characterization. This behavior confirms the performance reported in the polarization (Fig. 6).

Essentially, the EIS demonstrated a correlation between the type of dye used and the calculated charge transfer resistance.

The equivalent circuit under illumination consists of a series resistor

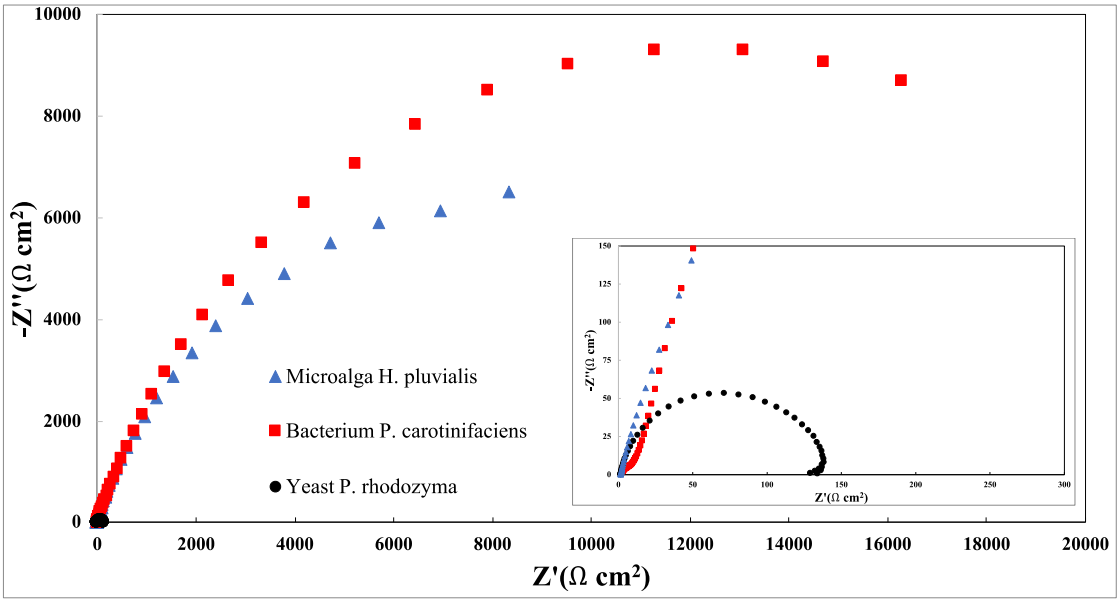

Fig. 7. Nyquist plots of DSSCs based on microalgae, bacterium and yeast. In the inset, however, an enlargement is shown to highlight the trend of the DSSCs based on *P. rhodozyma*.

Table 3
Values of series resistance and total resistance were calculated through Nyquist plot.

Dye	R_S (Ω cm^2)	R_T (Ω cm^2)
Microalga *H. pluvialis*	1.5	18,000
Bacterium *P. carotinifaciens*	1.5	22,000
Yeast *P. rhodozyma*	1.5	140

(ohmic resistor) connected in series with two components, each comprising a parallel combination of a resistor and a constant-phase element (CPE). The series resistor accounts for ohmic phenomena, while the R/CPE components are related to the properties of the electrode–electrolyte interface.“ Table 4 shows the values of individual circuit elements (Fig. 8) extracted from the fit to the experimental data. In detail, the component R2 related to the yeast confirms what is shown by the other characterizations (UV analyses, Fig. 3 and Nyquist plot, Fig. 7).

4. Conclusions

Astaxanthin is widely applied in several industrial fields, such as feed, food, cosmetics and pharmaceutical, mainly because of its biological properties. Thanks to its chemical structure as xanthophylls, it has been demonstrated to be suitable to be used as photosensitizer in DSSCs development due to the capability of binding the TiO_2 layer, providing interesting results as alternative application of this pigment besides its current industrial use.

In this study, focused on the employment of extracts obtained from three different astaxanthin producing microbial strains, it was possible to demonstrate that, when microbial extracts are used as photosynthesizes, it is important to clearly define the composition of the extracts, since the simultaneous presence of a mixture of dyes, resulting from the microbial metabolism, will affect the performance of the developed devices. In this study, in fact, even if all the microorganisms used are recognized and applied for astaxanthin production, only the bacterium *P. carotinifaciens* extract allowed to get the best DSSC performance, obtaining a PCE value of 0.36 % and a Jsc of 2.86 %, as consequence of the difference mixture of pigments detected in the extract; probably the occurrence in the *P. carotinefaciens* extract of an higher number of carotenoids bearing keto and hydroxyl groups and also the presence of astaxanthin in its free form (not esterified) having a 3S,3′S configuration, had a contribution to its best DSSC performance. Though the photovoltaic parameters of the devices implemented in this study are still low compared with those obtained by using synthetic dyes, these results constitute an important achievement towards the development of greener solar cells using microbial dyes.

Table 4
Values of circuital elements of Equivalent Electrical Circuit of investigated DSSCs.

Element	Units of measurement	Microalga *H. pluvialis*	Bacterium *P. carotinifaciens*	Yeast *P. rhodozyma*
R_S	Ω cm^2	1.5	1.5	1.5
R_1	Ω cm^2	75	25	33.5
Y_1 (CPE_1)	μS cm^{-2}s^n	315.6	377.1	489.5
n_1 (CPE_1)	–	0.741	0.651	0.884
R_2	Ω cm^2	17,925	21,975	105
Y_2 (CPE_2)	μS cm^{-2}s^n	7.4	6.1	76.8
n_2 (CPE_2)	–	0.915	0.931	0.911

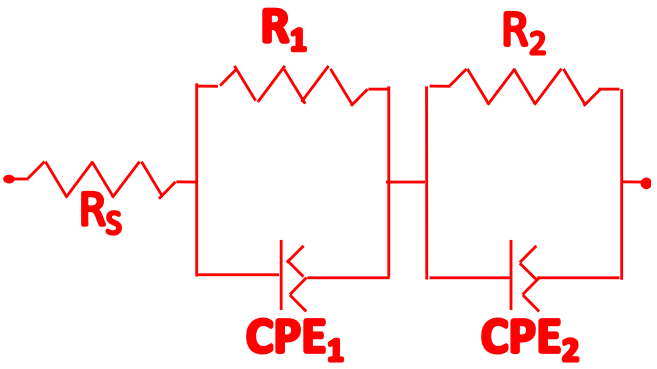

Fig. 8. Equivalent Electrical Circuit of investigated DSSCs used for parameter calculation.

Finally, it is important to highlight that *P. carotinifaciens* is a microorganism already used at industrial scale, representing this an important point to be evaluated, since the main problem connected to the implementation of microorganisms for dyes and pigments production is strictly connected to the microbial cultivation scalability.

Improving the efficiency of the DSSC-astaxanthin derived from *P. carotinifaciens*, by modifying the cultivation conditions, could result in a new application field of this microorganisms, scalable at industrial scale.

CRediT authorship contribution statement

Alessia Tropea: Writing – review & editing, Writing – original draft, Visualization, Validation, Resources, Methodology, Investigation, Formal analysis, Data curation, Conceptualization. **Donatella Spadaro:** Writing – review & editing, Writing – original draft, Visualization, Validation, Methodology, Investigation, Formal analysis, Data curation, Conceptualization. **Ilaria Citro:** Writing – review & editing, Writing – original draft, Visualization, Validation, Methodology, Investigation, Formal analysis, Data curation, Conceptualization. **Maurizio Lanza:** Writing – original draft, Investigation, Formal analysis. **Stefano Trocino:** Writing – original draft, Investigation, Formal analysis. **Roberta La Tella:** Writing – original draft, Investigation, Formal analysis. **Daniele Giuffrida:** Writing – original draft, Investigation, Formal analysis. **Cassamo U. Mussagy:** Writing – original draft, Resources. **Luigi Mondello:** Supervision, Resources, Project administration. **Giuseppe Calogero:** Supervision, Resources, Project administration.

Declaration of competing interest

The authors declare that they have no known competing financial interests or personal relationships that could have appeared to influence the work reported in this paper.

Acknowledgements

Authors thank the European Union (Next Generation EU), through the MUR-PNRR project NQSTI The National Quantum Science and Technology Institute (PE0000023) and POR H2 AdP MMES/ENEA with involvement of CNR and RSE, PNRR - Mission 2, Component 2, Investment 3.5 “Ricerca e sviluppo sull’idrogeno”, CUP: B93C22000630006; PRIN Project 2022 “Assessment of nano/microplastics impacts – PLASTACS”; project FOE 2022 project FutuRaw- The raw materials of the future from non-critical, residual and renewable sources and project. Finally, authors acknowledge Merck Life Science and Shimadzu Corporations for the continuous support.

Data availability

Data will be made available on request.

References

[1] N. Li, Q. Wang, J. Zhou, S. Li, J. Liu, H. Chen, Molecules 27 (2022) 3291, https://doi.org/10.3390/molecules27103291.
[2] R. Rollini, L. Falciola, S. Tortorella, Tetrahedron 113 (2022) 132758, https://doi.org/10.1016/j.tet.2022.132758.
[3] M.P. Narsing Rao, M. Xiao, W.J. Li, Front Microbiol. 8 (2017) 1–13, https://doi.org/10.3389/fmicb.2017.01113.
[4] R.S. Celedon, L.B. Díaz, Microorganisms 9 (4) (2021) 739, https://doi.org/10.3390/microorganisms9040739.
[5] P. Rajendran, P. Somasundaram, L. Dufossé, J. Mol. Struct. 1290 (2023) 135958, https://doi.org/10.1016/j.molstruc.2023.135958.
[6] C.K. Venil, L. Dufossé, P.D. Renuka, Front. Sustainable Food Syst. 4 (2020) 100, https://doi.org/10.3389/fsufs.2020.00100.
[7] A. Rodríguez-Mena, L.A. Ochoa-Martínez, S.M. Gonzalez-Herrera, O.M. Rutiaga-Quinones, R.F. Gonzalez-Laredo, B. Olmedilla-Alonso, Food Chem. 98 (2023) 133908, https://doi.org/10.1016/j.foodchem.2022.133908.
[8] K. Joshi, P. Kumar, R. Kataria, Process Biochem. 128 (2023) 190–205, https://doi.org/10.1016/j.procbio.2023.02.020.
[9] P. Sundararajan, S.P. Ramasamy, Sustain. Chem. Pharm. 37 (2024) 101353, https://doi.org/10.1016/j.scp.2023.101353.
[10] D. Zhou, Z. Fei, G. Liu, Y. Jiang, W. Jiang, C.S.K. Lin, W. Zhang, F. Xin, M. Jiang, Biotechnol. Adv. 74 (2024) 108392, https://doi.org/10.1016/j.biotechadv.2024.108392.
[11] A. Orona-Navar, I. Aguilar-Hernández, A. Cerdán-Pasarán, T. López-Luke, M. Rodríguez-Delgado, D.L. Cárdenas-Chávez, E. Cepeda-Pérez, N. Ornelas-Soto, Algal Res. 26 (2017) 15–24, https://doi.org/10.1016/j.algal.2017.06.027.
[12] Bartolotta and G. Calogero. Solar Cells and Light Management, 2020, 4, 107-161, ISBN 9780081027622. https://doi.org/10.1016/B978-0-08-102762-2.00004-5.
[13] G. Calogero, A. Bartolotta, G. Di Marco, D. Carlo, F. Bonaccorso, Chem. Soc. Rev. 44 (2015) 3244–3294, https://doi.org/10.1039/C4CS00309H.
[14] C.I. Higuera, V.L. Félix, F.M. Goycoolea, Crit. Rev. Food Sci. Nutr. 46 (2007) 185–196, https://doi.org/10.1080/10408690590957188.
[15] C.U. Mussagy, F.O. Farias, N.M. Bila, M.J.S.M. Giannini, J.F.B. Pereira, V.C. Santos-Ebinuma, A.J. Pessoa, Sep. Purif. Technol. 290 (2022) 120852, https://doi.org/10.1016/j.seppur.2022.120852.
[16] C.U. Mussagy, J.F.B. Pereira, L. Dufossé, Trends Biotechnol. 41 (8) (2023) 996–999, https://doi.org/10.1016/j.tibtech.2023.01.016.
[17] N.H.A. Manas, L.Y. Chong, Y.M. Tesfamariam, A. Zulkharnain, H. Mahmud, D.S. A. Mahmod, F.S.F.Z. Mohamad, N.I.W. Azelee, J. Biotechnol. 317 (2020) 16–26, https://doi.org/10.1016/j.jbiotec.2020.04.011.
[18] T. Montagni, P. Enciso, J.J. Marizcurrena, S. Castro-Sowinski, C. Fontana, D. Davyt, M.F. Cerdá, Environ Sustain 1 (2018) 89–97, https://doi.org/10.1007/s42398-018-0007-1.
[19] N. Ordenes-aenishanslins, G. Anziani-ostuni, M. Vargas-reyes, J. Alarcon, A. Tello, J.M. Perez-donoso, J. Photochem. Photobiol. b. 162 (2016) 707–714, https://doi.org/10.1016/j.jphotobiol.2016.08.004.
[20] A. Silva, R. Santos, C. Salazar, B. Lamilla, P. Pavez, R. Meza Hunter, L. Barrientos, Sol. Energy 181 (2019) 379–385, https://doi.org/10.1016/j.solener.2019.01.035.
[21] K. Deepankumar, A. George, G. Krishna, M. Ilamaran, N. Kamini, T. Senthil, S. Easwaramoorthi, N. Ayyadurai, ACS Sustain. Chem. Eng. 5 (2016) 72–77, https://doi.org/10.1021/acssuschemeng.6b01975.
[22] S.K. Srivastava, P. Piwek, S.R. Ayakar, A. Bonakdarpour, D.P. Wilkinson, V. G. Yadav, Small 2 (2018) 1–6, https://doi.org/10.1002/smll.201800729.
[23] Q. Fu, C. Zhao, S. Yang, J. Wu, Mater. Lett. 129 (2014) 195–197, https://doi.org/10.1016/j.matlet.2014.05.054.
[24] P. Hernandez-Velasco, I. Morales-Atilano, M. Rodríguez-Delgado, J.M. Rodríguez-Delgado, D. Luna-Moreno, F.G. Avalos-Alanís, J.F. Villarreal-Chiu, Dyes Pigm. 177 (2020) 108278, https://doi.org/10.1016/j.dyepig.2020.108278.
[25] A. Molaeirad, S. Janfaza, A. Karimi-Fard, B. Mahyad, Biotechnol. Appl. Biochem. (2014) 121–125, https://doi.org/10.1002/bab.1244.
[26] W. Li, Y. Pu, B. Ge, Y. Wang, D. Yu, S. Qin, Int. J. Hydrogen Energy 44 (2018) 1182–1191, https://doi.org/10.1016/j.ijhydene.2018.10.176.
[27] R. Mohammadpour, S. Janfaza, F. Abbaspour-Aghdam, Bioresour. Technol. 163 (2014) 1–5, https://doi.org/10.1016/j.biortech.2014.04.003.
[28] Z.H.H. Nurachman, W.R. Rahmaniyah, D. Kurnia, R. Hidayat, B. Prijamboedi, V. Suendo, E. Ratnaningsih, L.M.G. Panggabean, S. Nurbaiti, Algal Res. 10 (2015) 25–32, https://doi.org/10.1016/j.algal.2015.04.009.
[29] A. Orona-navar, I. Aguilar-hernandez, A. Cerdan-pasaran, T. Lopez-luke, Algal Res. 26 (2017) 15–24, https://doi.org/10.1016/j. algal.2017.06.027.
[30] N. Lammermann, F. Schmid-Michels, A. Weismann, L. Wobb, A. Hütten, O. Kruse, Sci. Rep. 9 (2019) 1–9, https://doi.org/10.1038/s41598-019-39344-6.
[31] R. Chauhan, A. Srivastava, P.M. Shirage, K. Bala, Sol. Energy 270 (2024) 112369, https://doi.org/10.1016/j.solener.2024.112369.
[32] A. Orona-Navar, I. Aguilar-Hernandez, T. Lopez-Luke, I. Zarazúa, A.V. Romero, J. P. Guerrero, N. Ornelas-Soto, J. Photochem. Photobiol. a: Chem. 388 (2020) 112216, https://doi.org/10.1016/j.jphotochem.2019.112216.
[33] S. Ito, T. Saitou, H. Imahori, H. Uehara, N. Hasegawa, Energy Environ. Sci. 3 (2010) 905–909, https://doi.org/10.1039/c000869a.
[34] J. Wook, T. Young, H. Seok, S. Han, S. Lee, K. Hee, Spectrochim Acta Part A Mol. Biomol. Spectrosc. 126 (2014) 76–80, https://doi.org/10.1016/j. saa.2014.01.122.
[35] A. Tropea, D. Spadaro, S. Trocino, D. Giuffrida, T.M.G. Salerno, J.P. Ruiz-Sanchez, J. Montañez, L. Morales-Oyervides, L. Dufossé, L. Mondello, G. Calogero, Photochem. Photobiol. Sci. (2024), https://doi.org/10.1007/s43630-024-00566-x.
[36] A. Spadaro, I. Tropea, S. Citro, D. Trocino, F. Giuffrida, L. Rigano, T. Morales-Oyervides, T. Brinkhoff, L. Tiso, G. Dufossé Calogero, L. Mondello, Dyes Pigments 229 (2024) 112311, https://doi.org/10.1016/j.dyepig.2024.112311.
[37] A. Orona-Navar, I. Aguilar-Hernandez, K.D.P. Nigam, A. Cerdan-Pasaran, N. Ornelas-Soto, J. Biotechnol. 332 (2021) 29–53, https://doi.org/10.1016/j.jbiotec.2021.03.013.
[38] C. Di Bari, C. Forni, A. Di Carlo, E. Barrajón-Catalán, V. Micol, F. Teoli, P. Nota, F. Matteocci, A. Frattarelli, E. Caboni, S. Lucioli, J. Photonics Energy 7 (2) (2017) 025503, https://doi.org/10.1117/1.JPE.7.025503.
[39] H.A. Maddah, V. Berry, S.K. Behura, Renew. Sustain. Energy Rev. 121 (2020) 109678, https://doi.org/10.1016/j.rser.2019.109678.
[40] N. Ahmad, J. Vunduk, A. Klaus, N.Y. Dahlan, S. Ghosh, F. Muhammad-Sukki, L. Dufossé, N.A. Bani, W.A.A.Q.I. Wan-Mohtar, Sustainability 14 (13894) (2022), https://doi.org/10.3390/su142113894.
[41] N. Prabavathy, R. Balasundaraprabhu, A.S. Kristoffersen, G. Balajia, S. Prasanna, K. Sivakumaran, M.D. Kannan, S.R. Erga, D. Velauthapillai, Optik 227 (2021) 166053, https://doi.org/10.1016/j.ijleo.2020.166053.
[42] M.J. Khan, A. Ahirwar, V. Sirotiya, A. Rai, S. Varjani, V. Vinayak, RSC Adv. 13 (2023) 22630, https://doi.org/10.1039/d3ra02927a.
[43] A.V. Caicedo Paz, F. Rigano, C. Cafarella, A. Tropea, L. Mondello, G.J.P. Martinez, M. Ahmad, A. Mustafa, F. Farias, A. Cordova, D. Giuffrida, L. Dufossè and C.U.

Mussagy. Separation and Purification Technology, 2024, 339, 126674. https://doi.org/10.1016/j.seppur.2024.126674.
[44] G. Calogero, J. Barichello, I. Citro, P. Mariani, L. Vesce, A. Bartolotta, A. Di Carlo, G. Di Marco, Dyes and Pigments, Volume 155, 2018, 75-83, ISSN 0143-7208.
[45] S.N. Karthick, K.V. Hemalatha, K.B. Suresh, C.F. Manik, S. Akshaya and H.J. Kim. Eds A. Pandikumar, K. Jothivenkatachalam and K. Bhojanaa, 2019, 1,1-16 https://doi.org/10.1002/9781119557401.ch1.
[46] Kalyanasundaram K, editor. Fundamental sciences, chemistry; 2010. 978-2-940222-36-0.
[47] G. Calogero, A. Sinopoli, I. Citro, G. Di Marco, V. Petrov, A.M. Diniz, A. Jorge Parola, F. Pina, Photochem. Photobiol. Sci. 12 (2013) 883–894, https://doi.org/10.1039/C3PP25347C.
[48] K. Holtin, M. Kuehnle, J. Rehbein, P. Schuler, G. Nicholson, K. Albert, Anal. Bioanal. Chem. 395 (2009) 1613–1622, https://doi.org/10.1007/s00216-009-2837-2.
[49] A.J. Meléndez-Martínez, C.M. Stinco, P. Mapelli-Brahm, Nutrients 11 (2019) 1093, https://doi.org/10.3390/nu11051093.
[50] H.K. Lichtenthaler, C. Buschmann, F4.3.1-F4.3.8.1, Curr. Protocol Food Anal. Chem. (2001), https://doi.org/10.1002/0471142913.faf0403s01.
[51] M. Tognetti, M. van Moliné Broock, D. Libkind, J. Basic Microbiol 53 (9) (2013) 766–772, https://doi.org/10.1002/jobm.201200274.
[52] C.M. Stinco, P. Mapelli-Brahm, Nutrients 11 (2019) 1093, https://doi.org/10.3390/nu11051093.
[53] D. Wei, Int. J. Mol. Sci. 11 (3) (2010) 1103–1113, https://doi.org/10.3390/ijms11031103.
[54] J. Bisquert, J. Phys. Chem. B 106 (2) (2002) 325–333, https://doi.org/10.1021/jp011941g.
[55] F.S.F.G. Belmonte, G.I.M. Sero, J. Bisquert, Sol. Energy Mater. Sol. Cells 87 (1–4) (2007) 117–131.
[56] Q. Wang, J.-E. Moser, M. Grätzel, J. Phys. Chem. B 109 (31) (2005) 14945–14953, https://doi.org/10.1021/jp052768h.
[57] A. Sacco. Renewable and Sustainable Energy Reviews, 2017, 79, 814-829, ISSN 1364-0321. https://doi.org/10.1016/j.rser.2017.05.159.
[58] D. Holzhacker, A. Ringleb and D. Schlettwein. Electrochimica Acta, 2024, 497, 2024, 144582, ISSN 0013-4686. https://doi.org/10.1016/j.electacta.2024.144582.
[59] S. Sarker, H.W. Seo and D.M. Kim. Chemical Physics Letters, 2013, 585, 193-197, ISSN 0009-2614. https://doi.org/10.1016/j.cplett.2013.08.101.
[60] S. Rudra, H.W. Seo, S. Sarker and D.M. Kim. Journal of Industrial and Engineering Chemistry, 2021, 97, 574-583, ISSN 1226-086X. https://doi.or g/10.1016/j.jiec.2021.03.010.